Tetrameric Stoichiometry of a Prokaryotic K^+ Channel[†]

Lise Heginbotham, Eric Odessey, and Christopher Miller*

Department of Biochemistry, Howard Hughes Medical Institute, Brandeis University, Waltham, Massachusetts

Received April 28, 1997; Revised Manuscript Received June 18, 1997[⊗]

ABSTRACT: Genes with sequences reminiscent of neuronal K^+ channels have recently been identified in prokaryotes. These putative K^+ channels appear to be integral membrane proteins, with multiple transmembrane sequences identified by hydrophobicity analysis and a sequence strikingly similar to the pore-lining "P-region" motif found in all known eukaryotic K^+ channels. This study examines the oligomeric state and stability in detergent micelles of SliK, a K^+ channel homologue from *Streptomyces lividans*. A synthetic gene for SliK was expressed at high levels in *Escherichia coli*, and the protein was purified. The predominant form of the protein runs in SDS−PAGE gels as an oligomer of the 19-kDa polypeptide, but harsh treatments such as heat or high pH convert this slowly-migrating material into monomeric form. A "mass-tagging" strategy developed to examine subunit stoichiometry shows that SliK is a homotetramer in SDS and dodecyl maltoside micelles. The tetrameric structure can be disrupted by P-region mutations known to prevent the functional expression of neuronal K^+ channels. The tetramer is remarkably stable, showing no conversion to the monomeric form after 14 days at room temperature. Although SliK-mediated cation flux activity was not observed, the tetrameric behavior of the protein argues that SliK may provide a system for a direct attack on the structure of a K^+ channel P-region sequence.

K^+ channels make up a ubiquitous, physiologically essential class of integral membrane proteins. These channels perform a multitude of biological roles and are gated by many different types of signals, but all display two defining characteristics. Functionally, K^+ channels contain an ion permeation pathway that is strongly selective for K^+ over both Na^+ and Ca^{2+}, the two other abundant biological cations. This selectivity is largely determined by a conserved "P-region" sequence of roughly 20 residues that line the pore (*1*−*5*). Structurally, K^+ channels share a common architecture: the voltage-gated K_v-type channels (and by implication all K^+ channels) are constructed according to a tetrameric "barrel−stave" plan in which four identical or homologous subunits surround the axially symmetric pore (*6*−*8*).

Many details of K^+ channel structure−function relations have been elaborated over the past few years, mainly because of opportunities offered by high-resolution electrophysiological analysis of genetically manipulated ion channels (*9*,*10*). It is frankly surprising that so much is known in this area since until recently, all K^+ channel studies were carried out in a complete structural vacuum. Low-resolution electron micrographs of K^+ channels (*11*,*12*) confirm their gross 4-fold symmetry, and the structures of soluble N-terminal "inactivation domains" have been described using NMR methods (*13*). However, the membrane-embedded core of the channel, including the ion conduction pore, remains elusive. K^+ channels have been stubbornly refractory to the protein-level biochemical attacks required for high-resolution structure determination. Even with heroic efforts, purification of K^+ channel protein from eukaryotic membranes has been achieved only in submilligram quantities (*12*,*14*−*18*), orders of magnitude lower than required for crystallization trials with integral membrane proteins. Furthermore, it is not yet known how to maintain long-term protein stability once the channels are solubilized in detergents; indeed, in one study, a substantial loss of functional activity was seen after only several hours (*19*).

The onrushing tsunami of genomic database information has uncovered K^+ channel P-region sequences in genes from many organisms not traditionally examined in electrophysiological work. Among these are several putative K^+ channels in prokaryotes, including *Escherichia coli* (*20*), *Streptomyces lividans* (*21*), and *Methanococcus jannaschii* (*22*). Recently, Schrempf and colleagues (*21*) isolated such a gene from *S. lividans*, achieved high-level expression of the protein in *E. coli*, and reported single-channel recordings of membranes doped with this protein. This *S. lividans* K^+ channel ("SliK") is much smaller than any known eukaryotic pore-forming subunit; it contains only 160 residues, and its hydrophobicity profile identifies two transmembrane α-helical stretches. These transmembrane sequences bear only modest similarity to those from eukaryotic K^+ channels, but the linker between them contains an unmistakable P-region motif like that found in K_v1 (*Shaker*-type) K^+ channels (67% identity, 81% similarity over 21 residues with no insertions or deletions). This combination of characteristics makes SliK a compelling target for a structural attack.

Before enthusiastically embracing SliK as a biochemically accessible model for the K^+ channels of electrically excitable cells, however, we consider it prudent to examine the physical state of the expressed protein in detergent micelles. This is particularly important since crystallization trials require that SliK must withstand extended periods in detergent solutions. Our results show that under these conditions SliK forms a stable homotetrameric structure, as expected for a properly assembled K^+ channel.

[†] Supported in part by NIH Grant GM-31768.
[⊗] Abstract published in *Advance ACS Abstracts,* August 1, 1997.

S0006-2960(97)00988-4 CCC: $14.00

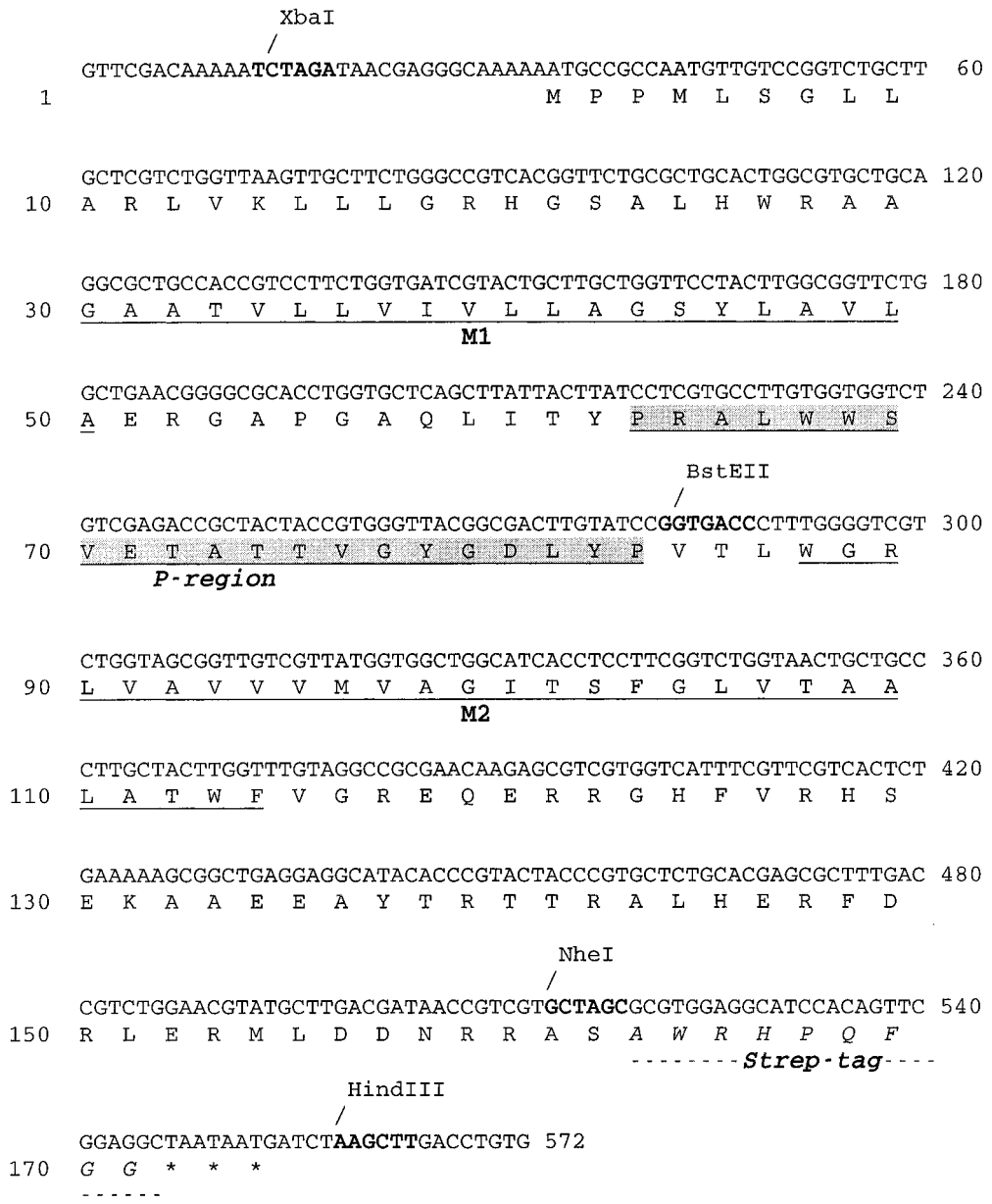

FIGURE 1: Sequence of the synthetic SliK gene. The sequence shown here carries a C-terminal strep-tag (italics) and two extra residues (A161 and S162) providing an *Nhe*I restriction site. The two transmembrane α-helical stretches (underlined) identified by hydropathy analysis are indicated as M1 and M2, and the P-region is shaded. Nucleotide numbering is shown on the right, and amino acid numbering is shown on the left. Throughout this paper, residue numbers refer to the sequence shown here.

EXPERIMENTAL PROCEDURES

Construction of a Synthetic Gene for SliK. The deduced amino acid sequence of the SliK polypeptide was reverse-translated using *E. coli* codon frequencies. The native protein sequence was altered at the carboxy-terminus by introducing two amino acids (A161, S162) followed by the 9-residue "strep-tag" sequence, which specifically binds to streptavidin (*23*). Oligonucleotides corresponding to the coding sequences 1−83, 121−200, 241−320, 361−440, and 486−572, and to the reverse of sequences 141−61, 260−181, 380−301, 505−421, and 572−543 (Figure 1) were synthesized and purified on acrylamide gels, and the gene was assembled according to established procedures (*24*). In brief, oligonucleotides were phosphorylated and annealed, and intervening sequence was filled in using Taq polymerase. After digestion with *Xba*I and *Hin*dIII, the gene was inserted in the pBluescript KS^- vector (Stratagene), and both strands were sequenced using the T7 and M13 primers. Polymerase errors were corrected using standard PCR mutagenesis methods, and the gene was transferred into pASK90, a derivative of the tetracycline-controlled expression vector pASK75 (*23*), kindly provided by Dr. Arne Skerra.

Modifications of SliK Gene. A hexahistidine tag (nucleotide sequence: CATCATCATCATCATCAT) was added immediately following the initial methionine residue using standard PCR mutagenesis. All constructs used here contained a hexahistadine sequence. In addition to the original SliK construct, which contained the strep-tag, we generated several variants with alternative C-terminal regions (Figure 1). A truncated construct, containing stop codons in place of a C-terminal recognition tag, was generated by introducing the sequence TGATG between the *Nhe*I and *Hin*dIII restriction sites. The hemagglutinin (HA) epitope was then inserted at the *Nhe*I site in this truncated gene (bases added: TATCCGTACGATGTCCCGGATTACGCC). In two other constructs, SliK-Rho8 and SliK-Rho45, C-terminal segments

of bovine rhodopsin were inserted between *Nhe*I and *Hin*dIII restriction sites. Both SliK-Rho genes include the terminal eight residues which make up the 1D4 epitope (*25*). For SliK-Rho8, the inserted sequence was generated from annealed oligonucleotides, and introduced the following sequence: GAGACCAGCCAAGTGGCGCCTGCCTAAT. With SliK-Rho45, the C-terminal 45 amino acids were transferred to the same region of SliK by generating a PCR fragment using a synthetic rhodopsin gene (*26*) as template with the 5′rho and 3′rho primers.

5′rho: GATAACCGTCGTGCTAGCGTCATCTAC-
ATCATGATGAACAAG

3′rho: CACAGGTCAAGCTTATTATTAGGCAGG-
CGCCACTTGGCTGGT

Point mutations at D80 and Y82 were generated by PCR mutagenesis of the region between *Xba*I and *Bst*EII, using Pfu polymerase. In each case, the mutated region was sequenced to verify the expected alterations and to rule out stray mutations.

Dicistronic Constructs for Bacterial Co-Expression. We generated dicistronic plasmids by linking two copies of the gene in the pASK90 plasmid with expression under the control of a single promotor region, similar to the strategy used with analogous vectors for the production of antibody fragments (*27*). Because each SliK subunit can be excised from the pASK90 plasmid using an *Xba*I/*Hin*dIII digest, construction of each dicistronic vector was a simple two-step procedure. First, an *Avr*II restriction site (cohesive end compatible with *Xba*I) was inserted just upstream from the *Hin*dIII site in the first gene by introducing the sequence AGCTCCTAGGACGTCAAGCT at the *Hin*dIII site. The second copy of the gene, excised from the pASK90 plasmid using *Xba*I and *Hin*dIII, was then inserted between *Avr*II and *Hin*dIII sites of the first vector.

Induction and Purification of SliK. A 6-mL overnight culture was inoculated with *E. coli* strain JM-83 (ATCC) transformed with pASK90:SliK. Cells were diluted into 300 mL of LB with 50 μg/mL ampicillin prewarmed to 37 °C. After reaching an OD_{550} of 0.5, expression was induced by the addition of 200 μg/L anhydrotetracycline (aTC, Acros Chemical Co.). Cells were harvested after 90 min and washed once with buffer A (100 mM NaCl, 5 mM KCl, 50 mM MOPS, pH 7.0). All subsequent procedures were carried out at 4 °C. Cells were resuspended in 12.5 mL of buffer A, and after the addition of protease inhibitors (final concentrations: PMSF, 1 mM; leupeptin, 2 μM; pepstatin, 2 μM) were disrupted by sonication. Unbroken cells and inclusion bodies were removed (12000*g*, 15 min), and membranes were pelleted from the supernatant (110000*g*, 45 min). Membranes were resuspended in buffer B (100 mM NaP_i, 5 mM KCl, pH 7.0) to a concentration of 2−8 mg/mL protein (assuming 1 OD_{280} = 1 mg/mL), extracted with 10 mM dodecyl maltoside (C_{12}M, CalBioChem) for 30 min and cleared by centrifugation (85000*g*, 45 min). When the protein was purified, imidazole was added to the extract (20−40 mM final concentration) and the pH was increased to 7.8. The extract was then incubated in batch with Ni-NTA agarose (Qiagen, 50 μL of matrix/mL of extract) for 90 min. The matrix was loaded into a column and washed (buffer B, 1 mM C_{12}M, 20−40 mM imidazole, pH 7.8) until $OD_{280} < 0.01$. The protein was eluted (buffer B containing 1 mM C_{12}M and 400 mM imidazole, pH 7.0). Protein concentration was determined with a Coomassie Plus protein assay (Pierce), relative to BSA standards diluted in the elution buffer.

SDS−PAGE and Western Blotting. Samples were diluted into Laemmli sample buffer containing 2% β-ME and were separated on SDS-containing acrylamide gels using standard Laemmli solutions (*28*). To visualize protein directly, gels were stained in a solution of Coomassie Brilliant Blue R-250. Alternatively, protein was transferred to nitrocellulose using a semi-dry transfer apparatus (Bio-Rad). Blots were blocked with 5% BSA for 15 min. For standard Western blots, a primary incubation with either anti-HA or 1D4 antibody (4 μg/20 mL of blocking buffer) for 30 min was followed by alkaline phosphatase (AP)-conjugated goat anti-mouse (Promega); blots were developed using NBT/BCIP reagents (Promega). To probe using streptavidin, the blocked blots were washed extensively and then incubated in avidin (16 μg/10 mL of buffer) to reduce background due to biotin-containing proteins. (The strep-tag does not bind with high affinity to avidin.) The blots were then incubated with AP-conjugated streptavidin (Promega, 20 μL/10 mL of buffer) and developed as described above for standard Western blots. Typically 20 μg of total protein, or 4 μg of purified protein, was loaded on each lane for Coomassie-stained gels or streptavidin blots, and 10−30 times less was loaded for HA and 1D4 Western blots.

Co-Immunoprecipitation. Samples of C_{12}M membrane extract (600 μL) were incubated with 48 μg of anti-HA antibody at 4 °C for 2 h. Following a 2-h incubation with 225 μL of ImmunoPure immobilized protein G (Pierce), the Sepharose was pelleted in a microcentrifuge and thoroughly washed (buffer B, 1 mM C_{12}M). Samples were resuspended in protein gel loading buffer and boiled for 15 min prior to loading.

RESULTS

Expression and Purification of SliK

We constructed a synthetic gene for SliK (Figure 1) on the basis of its deduced amino acid sequence (*21*). The *de novo* design strategy allowed us to incorporate several features to facilitate biochemical analysis. We used *E. coli* codon preferences and introduced several convenient restriction sites, including an *Nhe*I site near the 3′ end of the gene to permit the use of various epitopes for identification of SliK on immunoblots. When epitopes were not required, a stop codon was inserted after the *Nhe*I site to produce a product with two C-terminal residues added to the native protein sequence (see Experimental Procedures). A hexahistidine tag immediately following the initiator methionine enabled a simple Ni^{2+} affinity purification of SliK, as previously described (*21*); by a fortunate coincidence, the His-tag greatly increased SliK expression (data not shown). The synthetic SliK gene was cloned into a tetracycline-regulated expression vector.

Expression and purification of HA-tagged SliK, as monitored by Coomassie-stained SDS−PAGE gels and Western blots (Figure 2), were reproducible and straightforward. Whole *E. coli* extracts (lane 2) display little background reactivity to the anti-HA antibody prior to SliK induction. After induction (lane 3), two immunoreactive bands appear

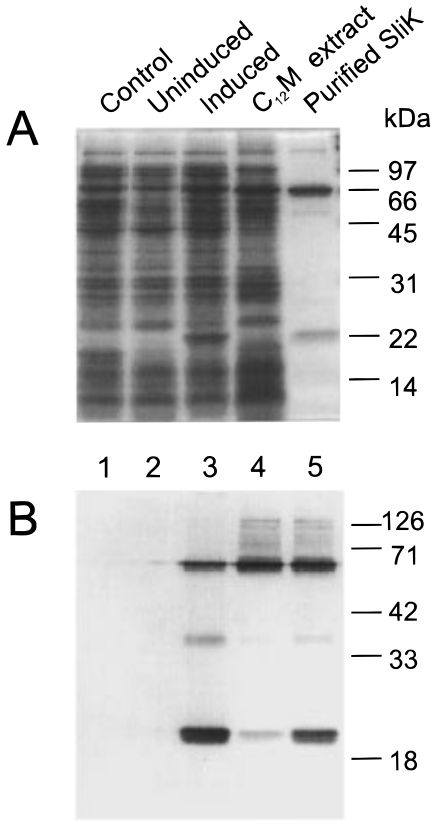

FIGURE 2: Induction and purification of HA-tagged SliK protein. The figure shows a 13% PAGE gel visualized with either Coomassie blue stain (A) or AP-conjugated streptavidin after transferring to nitrocellulose (B). The samples were generated from either HA-tagged SliK (lanes 2−5) or a construct lacking the epitope (lane 1). Crude extracts of total *E. coli* protein were prepared prior to (lane 2) or after (lanes 1 and 3) a 90-min induction. Membranes were enriched and subsequently solubilized using $C_{12}M$. The $C_{12}M$ extract (lane 4) was incubated with Ni^{2+} affinity matrix, and purified SliK was eluted from the matrix with imidazole (lane 5). Samples were run without prior heat treatment.

at apparent molecular weights of ~20 and ~60 kDa. Both of these bands, which we will refer to as "heavy" and "light," are readily visible in the Coomassie-stained gel of whole *E. coli* extracts. The light band runs as expected for the HA-tagged SliK polypeptide, but the heavy band also contains SliK protein. Both bands are absent from the immunoblot if the expressed SliK protein does not contain the HA epitope tag (lane 1) and are therefore SliK products rather than tetracycline-induced *E. coli* proteins. In the initial purification step, we solubilized the membrane fraction with the nonionic detergent $C_{12}M$. The heavy SliK species was greatly enriched by this step, becoming the major protein in the primary $C_{12}M$ extract (lane 4). The relatively low abundance of the light SliK band in the detergent extract suggests that this band represents denatured or incorrectly folded protein. Both forms of SliK are efficiently separated from other proteins by Ni^{2+}-affinity chromatography in the presence of $C_{12}M$ without addition of exogenous lipid (lane 5). We routinely obtain a yield of 1−3 mg/L of culture, as reported previously (*21*), with relative proportions of heavy and light bands similar to those shown in lane 5.

The idea that the heavy and light bands represent two different forms of SliK is verified by the observation that the heavy species may be converted into the light species under biochemically harsh conditions. Figure 3 summarizes experiments with SliK lacking an epitope tag; the majority

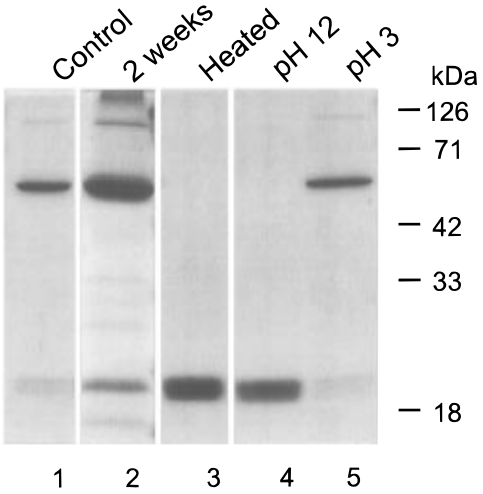

FIGURE 3: Stability of the heavy form of SliK. SliK protein lacking a C-terminal epitope tag was purified and subjected to various treatments. Lane 1, control; lane 2, after 2 weeks at room temperature; lane 3, 1 min, 100 °C; lane 4, 20 min, pH 12; lane 5, 20 min, pH 3. The gel was run and stained as in Figure 2A.

of the protein is in the heavy form. This heavy species is stable at room temperature in the SDS gel for at least an hour (lane 1) and in $C_{12}M$ micelles for at least two weeks (lane 2). The heavy form is completely converted to the light species by heating or exposure to high pH, but no such effect is seen with low-pH treatment (lanes 3−5). Since the light form of SliK migrates as expected for the 19-kDa polypeptide, these observations are most naturally explained if the light band represents denatured, monomeric protein. Several alternative hypotheses could readily account for the heavy form. For instance, it might be a folded, monomeric form of SliK not denatured by SDS which, because of its compact nature, binds a low amount of SDS and consequently runs slowly on the electrophoresis gel. Alternatively, it might represent an oligomeric form of SliK which is stable in the SDS gel. In this latter case, the sharpness of the band would suggest that the complex has a well-defined stoichiometry, since nonspecific aggregation of polypeptides often results in a ladder or smear of bands on SDS−PAGE. With either hypothesis, some degree of folded conformation would be needed to explain the anomalous migration of the heavy species. The question naturally arises: what is the oligomeric state of the heavy form of SliK?

Subunit Stoichiometry of SliK

We performed the obvious co-immunoprecipitation experiment to ask whether SliK subunits associate to form an oligomeric complex, but the results were ambiguous (Figure 4). Two subunits carrying different C-terminal epitopes (HA-tag and strep-tag) were either expressed individually or co-expressed using a dicistronic vector. Anti-HA antibody failed to precipitate any streptavidin-reactive protein when either subunit was expressed alone (lanes 1 and 2). Strep-tagged SliK was precipitated when the two subunits were co-expressed (lane 3), demonstrating the association of HA- and strep-tagged subunits. However, a signal (albeit weaker) also appeared when the HA- and strep-tagged subunits were expressed separately and mixed together (lane 4). This result, which may reflect nonspecific aggregation or exchange of subunits, undermines a clear interpretation of the co-immunoprecipitation seen in lane 3.

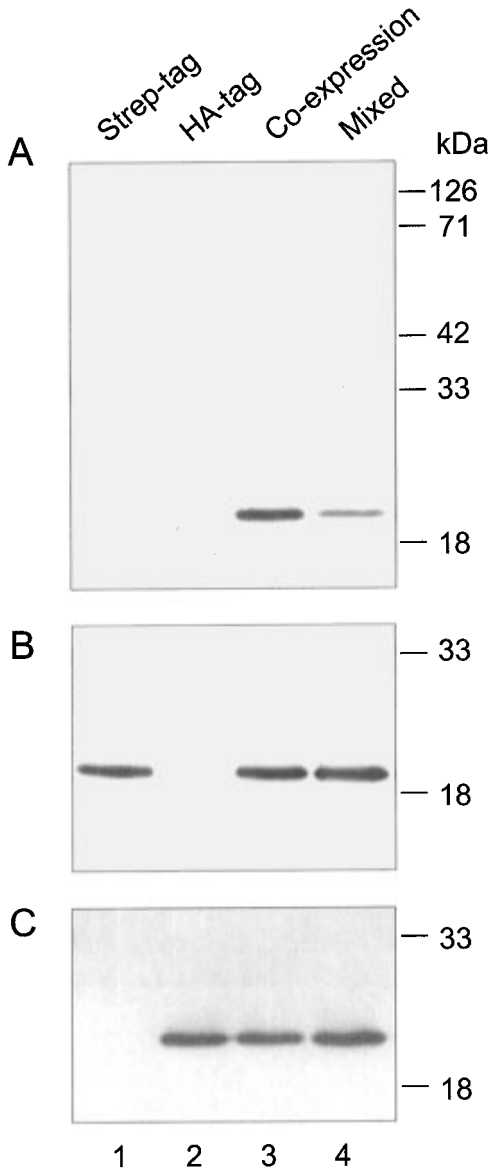

FIGURE 4: Co-immunoprecipitation of SliK subunits. Membrane extracts were prepared from *E. coli* expressing either the strep-tagged subunit (lane 1), the HA-tagged subunit (lane 2), or co-expressing both subunits (lane 3) using a dicistronic construct with HA- and strep-tagged subunits in the first and second positions, respectively. Lane 4 contains a mixture of the strep-tagged and HA-tagged extracts (lanes 1 and 2). (A) SliK was precipitated from membrane extracts with the anti-HA antibody and visualized using AP-conjugated streptavidin. Extracts were blotted with AP-conjugated streptavidin (B) or anti-HA antibody (C) to confirm that each extract contained the expected protein. Samples were heated prior to loading on a 13% SDS−PAGE gel, transferred to nitrocellulose, and visualized with either AP-streptavidin or anti-HA antibody.

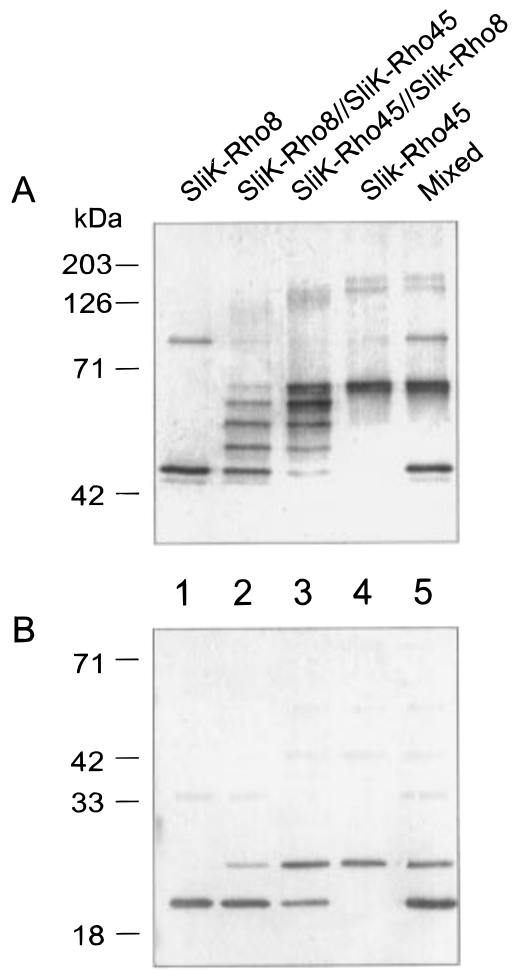

FIGURE 5: Western blot of mass-tagged SliK subunits. The small SliK-Rho8 (lane 1) or large SliK-Rho45 (lane 4) subunits were expressed individually, or were coexpressed using the two dicistronic constructs SliK-Rho8//SliK-Rho45 (lane 2) or SliK-Rho45//SliK-Rho8 (lane 3). In addition (lane 5), the separately expressed SliK-Rho8 and SliK-Rho45 subunits were mixed 2 h prior to loading. $C_{12}M$ extracts of the membrane protein were prepared from each sample, and aliquots were separated on a 7.5% gel (A). In parallel, samples were heat-treated and separated on a 13% gel (B). The 1D4 anti-rhodopsin antibody was used in both blots to visualize the protein. The amounts of samples loaded were adjusted empirically to obtain approximately equivalent signals in each lane.

As an alternative means to determine the subunit stoichiometry of SliK, we designed a protein-biochemical analogue of the "ball-tagging" method that has proven so useful in electrophysiological analysis of tetrameric K^+ channels (*7*,*8*,*29*,*30*). These experiments employed two forms of SliK proteins differing in the length of a C-terminal "mass-tag". The two constructs (SliK-Rho8, 20 kDa; SliK-Rho45, 24 kDa) carried either 8 or 45 C-terminal residues of rhodopsin. We expressed these two mass-tagged polypeptides either individually to form homo-oligomeric complexes or together in a dicistronic plasmid to form hetero-oligomers. Both polypeptides could be visualized on Western blots using the 1D4 epitope against the eight C-terminal residues of rhodopsin (*25*). When expressed individually, each type of protein shows the electrophoretic behavior expected for SliK (Figure 5A and 5B, lanes 1 and 4). Heavy forms are observed at apparent molecular weights of 50 and 65 kDa for SliK-Rho8 and SliK-Rho45, respectively. After heating in SDS, these proteins run at the molecular weights expected for the denatured polypeptides. In some cases, the heavy form shows a faint band running slightly faster than the predominant product; it is not clear whether this represents a proteolytic product or some conformational heterogeneity.

When the mass-tagged subunits are co-expressed, the heavy species splits into five bands (Figure 5A): two corresponding to the heavy forms of SliK-Rho8 and SliK-Rho45, and three novel bands migrating at positions intermediate between these parental proteins. Upon heating (Figure 5B), these five bands collapse into the two expected monomeric species. The figure also illustrates that the relative amounts of SliK-Rho8 and SliK-Rho45 expressed are influenced by the order of subunits within the dicistronic

plasmid. More protein is expressed from the first gene in the plasmid than from the second, a bias reflected in both the light and heavy products. When SliK-Rho8 is the upstream gene immediately following the promoter, the fast-migrating bands predominate in the heavy products, while the slow-migrating bands predominate if the gene order is reversed (Figure 5A). In both cases, the same five bands are observed, as if the hetero-oligomeric complex contains exactly four randomly associating subunits.

The experiment above exploits the combinatorial features of an oligomeric protein in order to infer stoichiometry. It argues that SliK forms a tetrameric complex. In light of this conclusion, Figures 2 and 3 show that nearly all the SliK protein purified after *E. coli* expression is tetrameric; the SliK complex runs somewhat below the expected molecular weight (~80 kDa) on SDS gels, as is sometimes observed with membrane proteins. Since it is firmly established that eukaryotic K^+ channels are tetrameric (*7*), this conclusion extends the homology between SliK and K^+ channels beyond primary sequence to the level of global structure.

Effects of P-Region Mutations on SliK Assembly

Ultimately, a meaningful purification of an ion channel protein requires reconstitution of function. So far, we have failed to observe $^{86}Rb^+$ transport in liposomes containing purified SliK (data not shown). This negative result raises the possibility that the tetramer we detect above is held together by a "multimerization domain" distant from the P-region, as suggested in *Shaker* K^+ channels (*31*), while the pore-forming part of the complex is disrupted, denatured, or otherwise unrepresentative of a functional K^+-selective channel. We therefore sought other indications of "channel-like" features of SliK that would gauge the structural integrity of the P-region sequence.

In properly folded neuronal K^+ channels, each of the four P-regions contributes to the lining of the conduction pathway. Since the pore constriction is narrow (~3 Å), the four pore-lining sequences of a properly assembled K^+ channel must be in close proximity. Thus, if the SliK tetramer adopts a channel-like conformation, we might expect the sequence of the SliK P-region to be a strong determinant of tetramer stability.

We examined this possibility by making point mutations at two sites in the P-region, D80 and Y82. The former is equivalent to a mutationally intolerant position, D447 in *Shaker* (*29*,*32*), while the latter is analogous to the external TEA-binding residue in eukaryotic K^+ channels (e.g., position 449 in *Shaker*), a position widely permissive of point mutations (*33*−*35*). Assembly of SliK is very sensitive to mutations at D80 (Figure 6). Although the conservative mutation D80E produced tetrameric SliK, only monomer was observed with A, N, or S substitutions. In contrast, at Y82 some nonconservative substitutions (T, V) did yield stable tetramers, while another (K) did not. In eukaryotic K^+ channels, many P-region mutations disrupt function, but the mechanisms by which this occurs are not known. Our results argue that in SliK, the P-region is critical for tetramerization. If this conclusion were to apply to eukaryotic K^+ channels as well, the P-region would join the two previously recognized tetramerization sequences, the N-terminal T1 domain (*31*,*36*) and the intramembrane association domain (*37*), as a crucial determinant of subunit assembly.

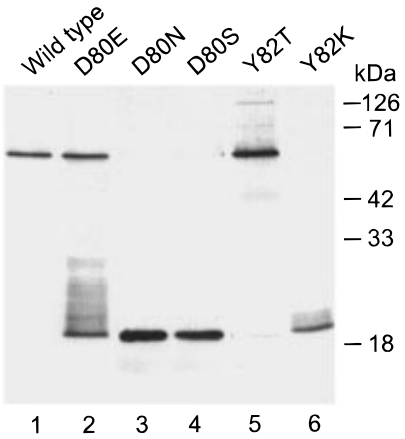

FIGURE 6: Tetramerization of SliK is affected by P-region mutations. Membranes were prepared from *E. coli* expressing the indicated strep-tagged SliK proteins, and were then extracted in $C_{12}M$. Samples were run on a 13% gel, transferred to nitrocellulose, and visualized with AP-conjugated streptavidin. In preliminary experiments with solubilized whole *E. coli* (data not shown), D80A and Y82V are similar in behavior to D80S and Y82T, respectively.

DISCUSSION

Our motivation in this study is to evaluate the suitability of a putative K^+ channel protein for direct structural investigation. The discovery of the SliK gene (*21*) has raised hopes for finally bridging the structural abyss that has prevented a thorough molecular understanding of ion channel mechanisms. The P-region sequence, which identifies SliK as a K^+ channel candidate, is impressively similar to that found in K^+ channels of electrically excitable membranes. The gene is readily expressed in *E. coli* at levels high enough to contemplate practicable production of purified protein in the 100-mg range. In addition, from studies in which single-channel fluctuations were observed in membranes containing SliK, Schrempf and colleagues (*21*) concluded that the expressed protein forms a functional ion channel.

Despite these hopeful signs, caution is warranted regarding the state of the purified SliK protein, and further experimental examination of the protein in micellar solution is needed. Our concerns stem largely from experience accumulated in attempts at high-level expression of eukaryotic K^+ channels. Mammalian and insect cell systems, both of which can be maneuvered to produce *Shaker*-type channels at high density (*12*,*19*,*38*), have been disappointing, with nonfunctional protein often predominating. Quantifying the activity of a purified ion channel is itself problematic, requiring techniques such as ligand binding or flux measurements to sample the entire population of channel protein. Single-channel analysis is a powerful method for characterizing ion channels in mechanistic detail, but it is poorly suited for surveying the bulk of protein in a biochemical preparation. The assay selects only those proteins that are functional but gives no information regarding the abundance of nonfunctional protein in the preparation. Added to this problem is the observation that partially denatured proteins or amphipathic peptides, when applied to phospholipid membranes, can produce channel-like current fluctuations.

As has been discussed in numerous contexts (*39*−*42*), verification of a purified channel preparation is achieved only when single-channel characteristics are combined with assays on the bulk population of protein. For these reasons, we do not consider single-channel recordings alone a definitive

demonstration of the functional competence of purified SliK. However, our failure to observe SliK-mediated ionic flux does not imply that the channel is improperly folded or otherwise debased; the activities of reconstituted membrane proteins are known to be sensitive to external variables such as membrane lipids, detergents, and aqueous ionic composition in ways that must be empirically determined for each system. Moreover, examples abound (*43*,*44*) in which auxiliary subunits or post-translational modifications are required for channel function, and a similar situation might apply here. These considerations prompted us to seek other evidence regarding the structural integrity of the protein. We therefore examined the oligomeric state and biochemical stability of SliK in micellar solution, conditions which the channel protein must ultimately experience in crystallization studies.

Many classical solution techniques, such as sedimentation and gel filtration, are available for investigating protein mass and size, which in turn reveal oligomeric state. These methods are generally reliable for well-behaved soluble proteins. However, with membrane proteins, interpretations of data from such experiments are nearly always vitiated by the uncontrolled amounts of lipid and detergent associated with the protein (*45*). Indeed, preliminary experiments in which we used size-exclusion chromatography on Superose-12 FPLC columns were uniformly ambiguous (data never to be shown). Because of these uncertainties, we chose to take an alternative approach that exploits the combinatorial characteristics of the oligomer.

The mass-tagging experiments introduced here show that SliK is a homotetramer in detergent micelles. These experiments, which reveal the five distinct mass-states of randomly assembled tetramers, are similar in spirit to the method used by Creighton (*46*) to count disulfide bonds in his early studies of protein folding and by Sakaguchi and colleagues (*47*) to evaluate cross-linking studies of tetrameric M2 channels from the influenza virus envelope. We have analyzed our mass-tagging experiments only qualitatively to provide a count of the heteromeric species; since the stability of the tetramer is affected by the length of the C-terminal tag, we cannot perform a detailed binomial analysis on the distribution of heterotetrameric SliK complexes. It is clear, however, that the distribution shifts according to the relative amounts of the two forms of SliK, and this result makes sense in terms of a binomial association of the subunits. SliK tetramers are remarkably stable, enduring for at least two weeks in mild detergent and even under conditions prevailing during SDS gel electrophoresis. This sort of association behavior is uncommon in membrane proteins but is not unprecedented (*48*−*51*).

Whereas our evidence for tetrameric assembly of SliK is direct, that for a "channel-like" tetramer is only circumstantial. In the absence of incontrovertible functional data, the relationship between the SliK tetramer and proper K^+ channel architecture must remain only suggestive. Nevertheless, the parallel effects of P-region mutations on SliK tetramerization and eukaryotic K^+ channel function are striking and suggest that these tetrameric proteins assume similar P-region conformations. Considering this evidence, we are optimistic about the value of SliK as an object of future structural study. It is a tantalizing fact that all six of the integral membrane proteins so far successfully analyzed by X-ray crystallographic methods are either from honorary prokaryotes (mitochondria and chloroplasts) or from prokaryotes themselves.

ACKNOWLEDGMENT

We thank D. Oprian and T. McKee for rhodopsin therapy and V. Suri, M. Maduke,* J. Mindell,* C. Deutsch, D. Pheasant, M. Schopperle, and E. Perozo for discussions and provocations. The acknowledgees indicated by the asterisks caused the authors equal aggravation. We are also particularly grateful to Dr. A. Skerra for providing the pASK90 expression vector.

REFERENCES

1. Yellen, G., Jurman, M., Abramson, T., and MacKinnon, R. (1991) *Science 251*, 939−942.
2. Hartmann, H. A., Kirsch, G. E., Drewe, J. A., Taglialatela, M., Joho, R. H., and Brown, A. M. (1991) *Science 251*, 942−944.
3. Heginbotham, L., Abramson, T., and MacKinnon, R. (1992) *Science 258*, 1152−1155.
4. Taglialatela, M., Drewe, J. A., Kirsch, G. E., de Biasi, M., Hartmann, H. A., and Brown, A. M. (1993) *Pflügers Archiv. 423*, 104−112.
5. Heginbotham, L., Lu, Z., Abramson, T., and MacKinnon, R. (1994) *Biophys. J. 66*, 1061−1067.
6. Christie, M. J., North, R. A., Osborne, P. B., Douglass, J., and Adelman, J. P. (1990) *Neuron 4*, 405−411.
7. MacKinnon, R. (1991) *Nature (London) 500*, 232−235.
8. MacKinnon, R., Aldrich, R. W., and Lee, A. W. (1993) *Science 262*, 757−759.
9. Miller, C. (1991) *Science 252*, 1092−1096.
10. Sigworth, F. J. (1994) *Q. Rev. Biophys. 27*, 1−40.
11. Li, M., Unwin, N., Stauffer, K. A., Jan, Y. N., and Jan, L. Y. (1994) *Curr. Biol. 4*, 110−115.
12. Spencer, R. H., Sokolov, Y., Li, H., Takenaka, B., Milici, A. J., Aiyar, J., Nguyen, A., Park, H., Jap, B., Hall, J. E., Gutman, G., and Chandy, K. G. (1997) *J. Biol. Chem. 272*, 2389−2395.
13. Antz, C., Geyer, M., Fakler, B., Schott, M. K., Guy, H. R., Frank, R., Ruppersberg, J. P., and Kalbitzer, H. R. (1997) *Nature (London) 385*, 272−275.
14. Rehm, H., and Lazdunski, M. (1988) *Proc. Natl. Acad. Sci. U.S.A. 85*, 4919−4923.
15. Parcej, D. N., and Dolly, J. O. (1989) *Biochem. J. 257*, 899−903.
16. Santacruz-Toloza, L., Perozo, E., and Papazian, D. M. (1994) *Biochemistry 33*, 1295−1299.
17. Garcia-Calvo, M., Knauss, H. G., McManus, O. B., Giangiacomo, K. M., Kaczorowski, G. J., and Garcia, M. L. (1994) *J. Biol. Chem. 269*, 676−682.
18. Scott, V. E. S., Rettig, J., Parcej, D. N., Keen, J. N., Findlay, J. B. C., Pongs, O., and Dolly, J. O. (1994) *Proc. Natl. Acad. Sci. U.S.A. 91*, 1637−1641.
19. Sun, T., Naini, A. A., and Miller, C. (1994) *Biochemistry 33*, 9992−9999.
20. Milkman, R. (1994) *Proc. Natl. Acad. Sci. U.S.A. 91*, 3510−3514.
21. Schrempf, H., Schmidt, O., Kummerlin, R., Hinnah, S., Muller, D., Betzler, M., Steinkamp, T., and Wagner, R. (1995) *EMBO J. 14*, 5170−5178.
22. Ketchum, K. A., Klenck, H.-P., White, O., and Ventner, J. C. (1997) *Biophys. J. 72*, A354.
23. Schmidt, T. G., and Skerra, A. (1993) *Protein Eng. 6*, 109−122.
24. Kammann, M., Laufs, J., Schell, J., and Gronenborn, B. (1989) *Nucleic Acids Res. 17*, 5404−5407.
25. MacKenzie, D., Arendt, A., Hargrave, P., McDowell, J. H., and Molday, R. S. (1984) *Biochemistry 23*, 6544−6548.
26. Ferretti, L., Karnik, S. S., Khorana, H. G., Nassal, M., and Oprian, D. D. (1986) *Proc. Natl. Acad. Sci. U.S.A. 83*, 599−603.
27. Skerra, A. (1994) *Gene 151*, 131−135.
28. Laemmli, U. K. (1970) *Nature (London) 227*, 680−685.

29. Lü, Q., and Miller, C. (1995) *Science 268*, 304−307.
30. Naranjo, D., and Miller, C. (1996) *Neuron 16*, 123−130.
31. Li, M., Jan, Y. N., and Jan, L. Y. (1992) *Science 257*, 1225−1230.
32. Kirsch, G. E., Pascual, J. M., and Shieh, C.-C. (1995) *Biophys. J. 68*, 1804−1813.
33. MacKinnon, R., and Yellen, G. (1990) *Science 250*, 276−279.
34. Heginbotham, L., and MacKinnon, R. (1992) *Neuron 8*, 483−491.
35. Kavanaugh, M. P., Hurst, R. S., Yakel, J., Varnum, M. D., Adelman, J. P., and North, R. A. (1992) *Neuron 8*, 493−497.
36. Shen, N. V., Chen, X., Boyer, M. M., and Pfaffinger, P. J. (1993) *Neuron 11*, 67−76.
37. Tu, L., Santarelli, V., Sheng, Z., Skach, W., Pain, D., and Deutsch, C. (1996) *J. Biol. Chem. 271*, 18904−18911.
38. Klaiber, K., Williams, N., Roberts, T. M., Papazian, D. M., Jan, L. Y., and Miller, C. (1990) *Neuron 5*, 221−226.
39. Miller, C., Garcia, A. M., and Bell, J. E. (1984) *Curr. Top. Membr. Transport 21*, 99−132.
40. Woodbury, D. J., and Miller, C. (1990) *Biophys. J. 58*, 833−839.
41. Bear, C. E., Li, C., Kartner, N., Bridges, R. J., Jensen, T. J., Ramjeesingh, M., and Riordan, J. R. (1992) *Cell 68*, 809−818.
42. Middleton, R. E., Pheasant, D. J., and Miller, C. (1994) *Biochemistry 33*, 13189−13198.
43. Inagaki, N., Gonoi, T., Clement, J. P., Namba, N., Inazawa, J., Gonzalez G., Aguilar-Bryan, L., Seino, S., and Bryan, J. (1995) *Science 270*, 1166−1170.
44. Krapivinsky, G., Gordon, E. A., Wickman, K., Velimirovic, B., Krapivinsky, L., and Clapham, D. E. (1995) *Nature (London) 374*, 135−141.
45. Reynolds, J. A., and Karlin, A. (1978) *Biochemistry 17*, 2035−2038.
46. Creighton, T. E. (1974) *J. Mol. Biol. 87*, 579−602.
47. Sakaguchi, T., Tu, Q., Pinto, L. H., and Lamb, R. A. (1997) *Proc. Natl. Acad. Sci. U.S.A. 94*, 5000−5016.
48. Fujii, J., Maruyama, K., Tada, M., and MacLennan, D. H. (1989) *J. Biol. Chem. 264*, 12950−12955.
49. Henry, G. D., and Sykes, B. D. (1990) *J. Mol. Biol. 212*, 11−14.
50. Lemmon, M. A., Flanagan, J. M., Treutlein, H. R., Zhang, J., and Engelman, D. M. (1992) *Biochemistry 31*, 12719−12725.
51. Arkin, I. T., Adams, P. D., MacKenzie, K. R., Lemmon, M. A., Brunger, A. T., and Engelman, D. M. (1994) *EMBO J. 13*, 4757−4764.

BI970988I